An Approach to Aerodynamic Design through Numerical Optimization

Howard P. Buckley, * and David W. Zingg †

Institute for Aerospace Studies, University of Toronto

4925 Dufferin St., Toronto, Ontario, M3H 5T6, Canada

A multipoint optimization approach is used to solve aerodynamic design problems encompassing a broad range of operating conditions in the objective function and constraints. The designer must specify the range of on-design operating conditions, the objective function to be minimized, a weighting function based on the mission or fleet requirements, and a set of performance and geometric constraints. Based on this designer input, a weighted integral objective function is developed. The numerical optimization problem is then formulated as a constrained multipoint problem with the weight assigned to each operating condition determined by a quadrature rule. The approach is illustrated with several design problems for transonic civil transport aircraft, and is extended to the formulation of aircraft range and endurance objective functions for use in the design of an unmanned aerial vehicle. The results demonstrate that the approach enables the designer to design an airfoil that is precisely tailored to the problem specification. Pareto fronts are presented as a means of providing the designer with information on trade-offs that can be used to guide the problem specification.

Nomenclature

C_d	coefficient of drag
C_l	coefficient of lift
$C^*_{l,max}$	lower bound on maximum lift coefficient constraint

*Research Engineer, Member AIAA, howard@oddjob.utias.utoronto.ca

†Professor, Canada Research Chair in Computational Aerodynamics, J. Armand Bombardier Foundation Chair in Aerospace Flight, http://goldfinger.utias.utoronto.ca/ dwz

$\mathcal{J}$	objective function
$\mathcal{Z}$	designer priority weighting function
$\mathcal{T}$	quadrature rule weights for integral approximation
M	Mach number
M_{ks}	estimate of maximum Mach number in the flow field given by the KS function
M_{max}	maximum Mach number in the flow field
M^*_{max}	upper bound on maximum Mach number constraint
W	aircraft weight
h	altitude
R	range
E	endurance
$\mathcal{R}$	range factor
$\mathcal{E}$	endurance factor
$\mathcal{R}'$	range factor, inverted integrand
$\mathcal{E}'$	endurance factor, inverted integrand
s	sound speed

I. Introduction

Design of an aerospace vehicle is a complex multidisciplinary problem. There are an enormous number of different operating conditions that must be accounted for. With experience the required number of operating conditions can be reduced, but it remains extremely large. Some of these operating conditions contribute to the overall objectives of the design, while others primarily impose constraints. The design problem is further complicated by the fact that the aircraft will fly a variety of missions, and the fleet profile cannot be precisely known. There are many other uncertainties, for example in the analyses, that necessitate a robust design and an understanding of trade-offs. An additional challenge is due to the fact that many of the operating conditions in the full flight envelope are expensive and time consuming to simulate accurately.

Based on the preceding description, it is clear that powerful tools will be needed to tackle such design problems and that we do not have such tools at present. Some of the desired properties of a design system include the following:

1. Must efficiently find an optimal solution and be robust enough to allow a thorough exploration of the design space.

2. Should be automated when designer intervention is not required and easy to interact

with when designer input is needed.

3. Should provide the designer with feedback regarding trade-offs and the implications of choices.

4. Must produce robust designs such that performance is insensitive to expected variance from optimal geometry and operating conditions.

5. Must be capable of incorporating the designer's priorities into the design.

We do not expect the design process based on such tools to proceed linearly from a well defined problem specification to a final design. Rather we expect the feedback from the design process to influence the problem formulation such that several iterations may be required. A brute force approach is unlikely to be feasible, and considerable ingenuity and expertise will be required to formulate the problem such that it is tractable.

In this paper, we take a step toward the development of an approach to optimization problems in which the objective function and constraints involve a wide range of operating conditions. We consider only one discipline, aerodynamics, and restrict our interest to two dimensions, i.e. airfoil design. Moreover, we consider only a small subset of operating conditions in the flight envelope and only a single configuration, a clean geometry. For a practical design there are numerous further considerations, including high lift, aerostructural trade-offs, aeroelasticity, and three-dimensional effects. Our objective is to apply our approach to sample problems of sufficient complexity to demonstrate its suitability for more complex problems.

Multipoint aerodynamic shape optimization can be used for a variety of purposes.[1–7] For example, Huyse et al.[4–6] have written a series of papers addressing robust design and design under uncertainty using a weighted integral approach based on probability density functions. However, there has been little research on the formulation of optimization problems that address a comprehensive set of design requirements, constraints, and operating conditions, which is the focus of this paper. Elias and Zingg[3] presented an automated technique for selecting sampling points and weights to achieve specified performance over a range of Mach numbers. Buckley et al.[7] took this a step further, solving an eighteen-point optimization problem including eight on-design operating conditions and ten off-design operating conditions. Here we present a significant improvement over our previous approach using a weighted integral to handle a broad range of on-design operating conditions in combination with several constraints based on off-design operating conditions. We apply the new approach to three design problems in order to demonstrate its effectiveness. Finally, we demonstrate how Pareto fronts can be used to provide the type of feedback the designer needs to reformulate the design problem if necessary.

II. Overview of Optima2D

Optima2D is a code for aerodynamic shape optimization developed by Nemec and Zingg[8,9] that employs a two-dimensional turbulent flow solver. The compressible Reynolds-averaged Navier-Stokes equations are solved at each design iteration with a Newton-Krylov method in which the linear system arising at each Newton iteration is solved using the generalized minimal residual method (GMRES) preconditioned with an incomplete lower-upper (ILU) factorization with limited fill. Spatial derivatives in the governing equations are discretized using second-order centered finite differences with added scalar numerical dissipation. Eddy viscosity is computed using the one-equation Spalart-Allmaras turbulence model.

The airfoil geometry is parametrized using B-spline control points. The vertical coordinates of these control points are design variables, thus allowing alterations to the baseline shape. For lift-constrained drag minimization problems, the design variables are B-spline control points, and the angle of attack is computed as part of the flow solution in order to meet the lift constraint. For lift maximization problems, the angle of attack is a design variable in addition to the B-spline control points.

Gradients of objective and constraint functions that are dependent on the flow solution are calculated using the discrete-adjoint method; the adjoint equation is solved using preconditioned GMRES. Function and gradient evaluations are passed to the optimization algorithm, which determines how to modify the design variables in order to solve the optimization problem. At each design iteration, the grid around the updated airfoil shape is perturbed using a simple algebraic grid movement technique. The constrained optimization algorithm SNOPT developed by Gill, Murray, and Saunders[10] uses a sequential quadratic programming method that obtains search directions from a sequence of quadratic programming (QP) subproblems. Each QP subproblem minimizes a quadratic model of a Lagrangian function which is used to represent the objective function subject to linearized constraints.

III. Description of Aircraft Design Problems

A. Design Problem 1

1. Objective Function at On-Design Operating Conditions

A design problem considered previously by Buckley et al.[7] was based on a design specification for a hypothetical aircraft intended to be used as a transonic civil transport vehicle. In this work, we revisit this design problem and use the weighted integral approach to obtain optimal solutions for several test cases. Regions of the flight envelope considered for this design problem include cruise, dive, and low-speed conditions. These flight envelope regions span a range of values for Mach number, aircraft weight, and altitude. The performance

Design Point	Reynolds Number	Mach Number	Lift Coefficient	Operating Condition	Off-Design Constraint
1	28.88×10^6	0.76	0.20	dive	$M_{max} \leq 1.35$
2	28.88×10^6	0.76	0.11	dive	$M_{max} \leq 1.35$
3	28.88×10^6	0.76	0.33	dive	$M_{max} \leq 1.35$
4	28.88×10^6	0.76	0.18	dive	$M_{max} \leq 1.35$
5	19.62×10^6	0.76	0.32	dive	$M_{max} \leq 1.35$
6	19.62×10^6	0.76	0.17	dive	$M_{max} \leq 1.35$
7	19.62×10^6	0.76	0.52	dive	$M_{max} \leq 1.35$
8	19.62×10^6	0.76	0.28	dive	$M_{max} \leq 1.35$
9	11.8×10^6	0.16	-	low-speed	$C_{l,max} \geq 1.60$
10	15.0×10^6	0.20	-	low-speed	$C_{l,max} \geq 1.60$

Table 1. Off-design constraints and operating conditions for Design Problem 1

goal for the optimization is to minimize mean fuel consumption for the aircraft over the cruise flight envelope. It is achieved by minimizing an objective function defined as the integral of C_d over the range of specified cruise operating conditions. The aircraft weight ranges from 60,000 to 100,000 lbs, its cruise Mach number ranges from 0.78 to 0.88, and its cruise altitude ranges from 29,000 to 39,000 feet. C_l values corresponding to these operating conditions range from 0.27 to 0.58. The wings of the aircraft are swept at 35 degrees and have an area of 1000 square feet. Due to the wing sweep angle, the effective Mach number range is from 0.64 to 0.72.

2. Constraints at Off-Design Operating Conditions

In addition to optimizing performance over a range of cruise conditions, a set of constraints at dive and low-speed operating conditions is specified. Table 1 summarizes this set of off-design operating conditions and corresponding constraints. Off-design points 1-8 are associated with a safety requirement for maneuverability under dive conditions. The dive condition Mach number is 0.93, making the effective Mach number 0.76 accounting for the sweep angle. The endpoints of the range of aircraft weights and altitudes are considered together with two load factors, 0.7 and 1.3 at each combination of aircraft weight and altitude for a total of eight dive conditions. At each extreme of the aircraft weight range the load factors produce two lift requirements. In turn these lift requirements taken at each extreme of the altitude range are used to compute corresponding lift coefficients for the dive conditions. Similarly, the dive condition Reynolds Numbers correspond to the two extremes of the altitude range. The dive maneuverability requirement is achieved by keeping shock strengths modest under these conditions. This is imposed by requiring that the Mach numbers upstream of shocks are less than or equal to 1.35.

The final two operating points reflect a requirement to be able to achieve an adequate

Design Point	Reynolds Number	Mach Number	Lift Coefficient	Operating Condition	Off-Design Constraint
1	30.45×10^6	0.80	0.30	dive	$M_{max} \leq 1.35$
2	30.45×10^6	0.80	0.16	dive	$M_{max} \leq 1.35$
3	30.45×10^6	0.80	0.47	dive	$M_{max} \leq 1.35$
4	30.45×10^6	0.80	0.26	dive	$M_{max} \leq 1.35$
5	21.39×10^6	0.80	0.48	dive	$M_{max} \leq 1.35$
6	21.39×10^6	0.80	0.26	dive	$M_{max} \leq 1.35$
7	21.39×10^6	0.80	0.76	dive	$M_{max} \leq 1.35$
8	21.39×10^6	0.80	0.41	dive	$M_{max} \leq 1.35$
9	11.8×10^6	0.16	-	low-speed	$C_{l,max} \geq 1.60$
10	15.0×10^6	0.20	-	low-speed	$C_{l,max} \geq 1.60$

Table 2. Off-design constraints and operating conditions for Design Problem 2

maximum lift coefficient at low speed conditions. For operating condition 9, the altitude is sea level, the weight is 60,000 lbs, and the effective Mach number is 0.16. For operating point 10 the weight is 100,000 lbs, and the effective Mach number is 0.20. The low-speed requirement specifies that the maximum attainable lift coefficient under these conditions is at least 1.778[a].

B. Design Problem 2

A second design problem is considered for a faster, heavier aircraft. For Design Problem 2, the aircraft weight ranges from 100,000 to 160,000 lbs, its cruise Mach number ranges from 0.88 to 0.94, and its cruise altitude ranges from 29,000 to 39,000 feet. C_l values corresponding to these operating conditions range from 0.40 to 0.72. The aircraft wings are swept at 35 degrees and have an area of 1000 square feet. Taking into account the wing sweep, the effective Mach number range is from 0.72 to 0.77. As with Design Problem 1, the performance goal is to minimize average fuel consumption for the aircraft. This is achieved by minimizing the integral of C_d over the range of specified cruise operating conditions.

While the two off-design constraints at low-speed operating conditions are the same as for Design Problem 1, the eight off-design constraints at dive operating conditions correspond to the increased aircraft weight, a higher dive condition Mach number of 0.98, and load factors of 0.7 and 1.3. The effective dive condition Mach number is 0.80 accounting for the sweep angle. Table 2 summarizes the off-design constraints and operating conditions for Design Problem 2.

[a]The optimization procedures applied to the test cases in this work are demonstrated on a mesh of moderate density. Using a lower target lift coefficient of 1.60 on this mesh yields a lift coefficient of at least 1.778 on a fine mesh used for accurate performance evaluation. See the appendix for further explanation of the off-design constraint values used with moderate grid densities suitable for optimization problems.

C. Design Problem 3

Design problem 3 is a departure from the first two design problems. Here we consider the design of an unmanned aerial vehicle (UAV). The design specifications are based on a UAV intended for high-altitude-long-endurance missions. The aircraft weight ranges from 13,349 to 26,751 lbs. The aircraft has an unswept wing spanning 115 feet, and a wing area of 1000 square feet. It is expected to fly over a range of subsonic speeds from Mach 0.35 to 0.50 at an altitude of 60,000 feet. Reynolds numbers at these operating conditions range from four to six million. Design objectives for this type of aircraft differ significantly from those applicable to a transonic civil transport aircraft exemplified by design problems 1 and 2. For this aircraft, endurance is a significant design consideration as well as range. The two competing goals of maximizing range and endurance performance will be considered. Given that aircraft range and endurance are defined as integrals of aerodynamic quantities over a range of aircraft weights, the integral approach used to quantify these performance attributes as objective functions described in Section IV below is well suited to this design problem.

IV. Integral Formulation of Objective Functions

A. Minimizing Fuel Consumption at Prescribed Cruise Conditions

Given the design objective of reducing fuel burn over a range of cruise operating conditions, an objective function may be defined as the integral of C_d over the range of interest. Huyse and Lewis[4] proposed a weighted integral approach for the purpose of solving robust optimization problems where the design objective is to desensitize aerodynamic performance of a shape to variability about some operating condition. In their approach to robust optimization, a weighting function represents the statistical variance of the prescribed operating condition. We apply the concept of a weighted integral to design problems in which a range of Mach numbers M, aircraft weights W, and cruise altitudes h are considered. A weighting function is utilized that allows the designer to prioritize the importance of operating conditions, e.g. based on mission requirements of the aircraft. The weighted integral is defined as

$$\int_{h_1}^{h_2}\int_{W_1}^{W_2}\int_{M_1}^{M_2} C_d\left(M,W,h\right)\mathcal{Z}\left(M,W,h\right)\,dM\,dW\,dh \tag{1}$$

where C_d is a function of M, W, and h, and $\mathcal{Z}$ is a weighting function based on the priorities of the designer that may also be a function of M, W, and h. In order to demonstrate the use and impact of $\mathcal{Z}$, test cases presented in this work use two different weighting functions. The first is simply $\mathcal{Z}_1 = 1$, i.e. all conditions are equally weighted. The second weighting

function is a function of M only, given by

$$\mathcal{Z}_2(M) = e^{a(M-M_1)} \quad \text{with} \quad a = \frac{\ln(20)}{M_2 - M_1} \tag{2}$$

This function is defined such that $\mathcal{Z}_2(M_1) = 1$ and $\mathcal{Z}_2(M_2) = 20$ with $M_1 < M_2$, which places twenty times more weight on the high end of the Mach range than the low end. This weighting function is an example of one that would be suitable for the design of an aircraft or fleet of aircraft that will fly predominantly at $M = M_2$. We wish to emphasize that the choice of weighting function $\mathcal{Z}$ is dictated by the intended mission of the aircraft.

The objective function to be minimized is an approximation of the weighted integral (1) given by

$$\mathcal{J} = \sum_{i=1}^{N_M} \sum_{j=1}^{N_W} \sum_{k=1}^{N_h} \mathcal{T}_{i,j,k}\, C_d(M_i, W_j, h_k)\, \mathcal{Z}(M_i, W_j, h_k)\, \Delta M \Delta W \Delta h \tag{3}$$

where N_M, N_W, and N_h are the numbers of quadrature points used in M, W, and h respectively, and ΔM, ΔW, and Δh are the corresponding spacings between quadrature points. The $\mathcal{T}_{i,j,k}$ are the weights used to approximate the integral using a quadrature rule. At each quadrature point, drag minimization is subject to a lift constraint $[C_l = C_l^*]_{i,j,k}$. The accuracy of the integral approximation is dependent on the number of quadrature points used in its evaluation and the quadrature rule used. The trapezoidal rule is used in the present examples. To clarify the definition of $\mathcal{T}$, the trapezoidal quadrature weights used to approximate the integral of a single-variable function are $\mathcal{T} = [\frac{1}{2}, 1, ..., 1, \frac{1}{2}]$. For functions of more than one variable, as in our case, the trapezoidal quadrature weights have a similar form corresponding to the number of function variables.

B. Maximizing Aircraft Range and Endurance

Aircraft range is the maximum distance that can be traversed for a given payload weight. Similarly, aircraft endurance refers to the maximum amount of time that an aircraft can remain aloft carrying a specified payload. Considerations such as labour costs and passenger comfort associated with flight time place importance on faster operating speeds for civil transport aircraft whereas time available for data collection and area coverage, often without regard for operating speed, can be typical considerations when designing a UAV. In the absence of constraints on operating speed, the designer is free to choose an operating speed that best achieves the goal of maximizing either range or endurance. It should be noted that for a given aircraft, maximum range and endurance occur at different speeds. It follows that in addition to geometric design variables which enable manipulation of an aerodynamic shape, the Mach number must also be treated as a design variable when either aircraft range or endurance are to be optimized.

The equations for range and endurance, respectively, of an aircraft with jet propulsion can be expressed in integral form as

$$R = \int_{W_1}^{W_2} \frac{(sM)}{\text{TSFC}} \frac{C_l}{C_d} \frac{dW}{W} \tag{4}$$

$$E = \int_{W_1}^{W_2} \frac{1}{\text{TSFC}} \frac{C_l}{C_d} \frac{dW}{W} \tag{5}$$

where TSFC is the thrust-specific fuel consumption of the jet engines, s is the speed of sound, W_2 is the aircraft maximum takeoff weight, and W_1 is the maximum takeoff weight minus fuel weight. The evaluation of these integrals to obtain analytic expressions for range and endurance is dependent on which quantities inside the integral vary with aircraft weight W. For example, the Breguet range equation can be derived from (4) if one assumes that M, TSFC, and $\frac{C_l}{C_d}$ are constant over the duration of the flight. In practice, for this set of assumptions to hold, an aircraft must employ a cruise-climb flight schedule such that the plane gains altitude as its fuel weight decreases over the duration of the flight to maintain constant $\frac{C_l}{C_d}$. By assuming that the UAV flies at a constant altitude and speed, and TSFC is constant, simplified integrals that are proportional to range and endurance are obtained:

$$\mathcal{R} = \int_{W_1}^{W_2} \frac{MC_l}{C_d}\, dW \tag{6}$$

$$\mathcal{E} = \int_{W_1}^{W_2} \frac{C_l}{C_d}\, dW \tag{7}$$

$\mathcal{R}$ and $\mathcal{E}$ are referred to as range and endurance factors respectively. This requires that $\frac{C_l}{C_d}$ remain inside the integral since at constant speed and altitude, C_l and C_d vary with W. In order to maximize range or endurance, we wish to minimize modified versions of $\mathcal{R}$ or $\mathcal{E}$ with inverted integrands given by

$$\mathcal{R}' = \int_{W_1}^{W_2} \frac{C_d}{MC_l}\, dW \tag{8}$$

$$\mathcal{E}' = \int_{W_1}^{W_2} \frac{C_d}{C_l}\, dW \tag{9}$$

For a range optimization problem, the objective function is defined as an approximation of the integral $\mathcal{R}'$ given by

$$\mathcal{J} = \frac{\Delta W}{M} \sum_{j=1}^{N_W} \mathcal{T}_j \left[\frac{C_d}{C_l}\right]_j \tag{10}$$

where ΔW is the spacing between quadrature points over the range of aircraft weights $W_2 - W_1$. Note that while M is assumed to be constant in the calculation of range, it is treated as a design variable in the formulation of the range- and endurance-maximization optimization problems. The objective function for an endurance optimization problem is

derived in a similar fashion.

Integral formulations of the range and endurance objective functions are special cases of the more general weighted integral objective function described in the previous section. In particular, the assumptions of constant speed and altitude required for evaluation of integrals 6 and 7 leave only a range of aircraft weights to consider in the objective function. Also, the use of a designer-priority weighting function is not applicable under these circumstances as preference should not be given to any specific aircraft weight.

V. Multipoint Optimization Problem Setup

This description of optimization setup parameters applies to the cases presented in subsequent sections. The airfoil geometry is parametrized using 15 B-spline control points. One control point is frozen at the leading edge and two at the trailing edge. The remaining 12 control points are designated as design variables and are split evenly between the top and bottom airfoil surfaces. Thickness constraints of 1% chord and 0.2% chord are imposed at 95% chord and 99% chord respectively to prevent trailing edge crossover. The latter is typically inactive once convergence is achieved. The area of the optimal geometry is constrained to be at least the area of the initial geometry. For Design Problems 1 and 3, the RAE 2822 airfoil is used as the initial geometry. For Design Problem 2, an airfoil with a thickness to chord ratio of 10.5% is used as the initial geometry. In all cases, the base grid has a C topology with 289 nodes in the streamwise direction and 65 nodes in the normal direction; the off-wall spacing is 2×10^{-6} chord. It was created using the RAE 2822 airfoil geometry. See the appendix for details on the impact of the number of design variables and grid size.

For Design Problems 1 and 2, off-design points described in Tables 1 and 2 representing dive conditions are subject to the constraint that the maximum Mach number in the flow field not exceed 1.35. The maximum Mach number function is not continuous with respect to the design variables and therefore cannot be handled directly by SNOPT. To address this issue we use the Kreisselmeier-Steinhauser (KS) function[11] as a means to aggregate Mach number constraints evaluated at all nodes in the flow field into a single composite function that is continuously differentiable. M_{ks} represents a conservative estimate of the maximum Mach number in the flow field based on the KS function. Therefore, M_{max} constraints defined as $M^*_{max} - M_{max} > 0$, where the upper bound on the constraint is $M^*_{max} = 1.35$, translate to $M^*_{ks} - M_{ks} > 0$, where the upper bound on the constraint is $M^*_{ks} = 1.50$. This value of M^*_{ks} produces $M_{max} < 1.35$ at the optimal solution. An explanation of the determination of M^*_{ks} is provided in the appendix. Off-design points 9 and 10 in Tables 1 and 2 represent constraints at low-speed operating conditions such that $C_{l,max} - C^*_{l,max} > 0$, where the lower bound on the constraint is $C^*_{l,max} = 1.60$. The optimization procedures applied to the test

cases in this work are demonstrated on a mesh of moderate density. Using a lower target lift coefficient of 1.60 on this mesh yields a lift coefficient of at least 1.778 on a fine mesh used for accurate performance evaluation. See the appendix for further explanation of the off-design constraint values used with moderate grid densities suitable for optimization problems.

The flow solver described in Section II is used to evaluate airfoil performance in all cases. Given studies of the flow solver's accuracy performed by Zingg et al.,[12,13] the grids used can be expected to predict lift coefficients accurate to within 1% and drag coefficients to within 5% for attached and mildly separated flows, including both numerical and physical model error.

VI. Results

A. Comparison of Weighting Functions

The weighted integral approach described in Section IV-A is applied to Design Problems 1 and 2 described in Sections III-A and III-B. Optimizations are performed with the two weighting functions described in Section IV-A to illustrate their influence on the design problem solution. The first assigns equal weight to all operating conditions, the second prioritizes operating conditions such that weight increases exponentially with Mach number. For each design problem two additional optimizations are performed using the weighting functions described above but excluding the off-design constraints summarized in Tables 1 and 2. This demonstrates the extent to which on-design performance is penalized as a result of the need to satisfy the off-design constraints. In order to simplify the test cases and reduce computational expense, a constant cruise altitude of 39,000 feet is used for Design Problems 1 and 2; however a range of altitudes can be easily accommodated by the weighted integral approach. For each case the integral is approximated using the trapezoidal rule with 25 integration points evenly spaced over the range of cruise Mach numbers and aircraft weights. The solutions to Design Problems 1 and 2 satisfy the Karush-Kuhn-Tucker[14] optimality conditions for a constrained optimization problem to within a tolerance of 1×10^{-6}. Measures of optimization convergence versus SNOPT major iterations for the equal weighting case are shown in Figure 1. The SNOPT merit function is an augmented Lagrangian of the constrained optimization problem. In Figure 1 it is normalized by its initial value. Figure 2 gives a comparison of aerodynamic performance between the optimal solutions obtained with each weighting function. It shows the average C_d over the range of aircraft weights as a function of Mach number, where each data point represents the integral of C_d over the range of aircraft weights divided by $(W_2 - W_1)$, i.e. the average value of C_d over the associated range of lift coefficients at a fixed Mach number. A comparison of the optimal airfoil geometries obtained in each case is shown in Figure 3.

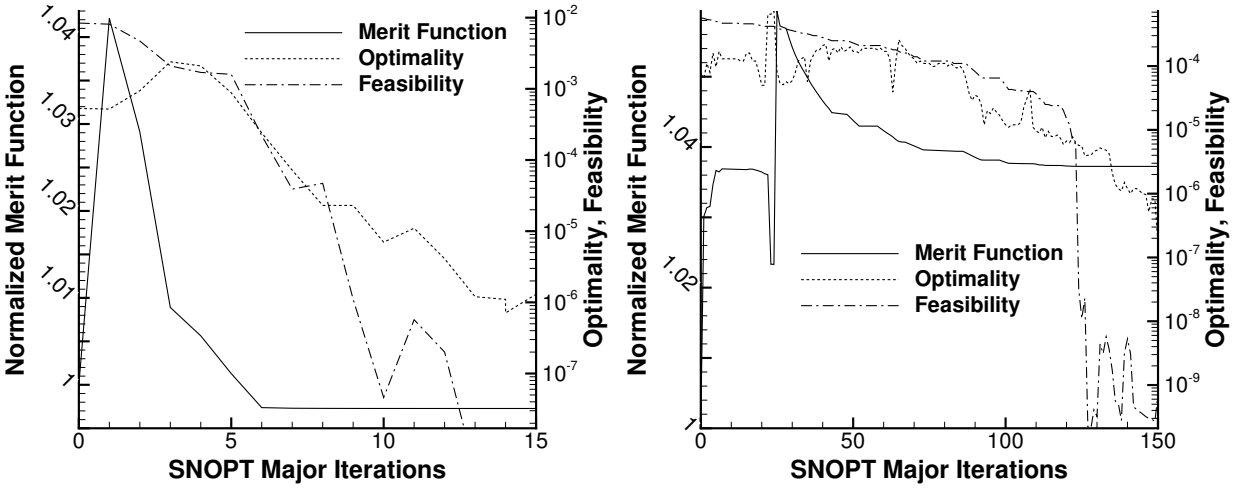

(a) Design Problem 1 (b) Design Problem 2

Figure 1. Optimization convergence histories for the equal weighting case

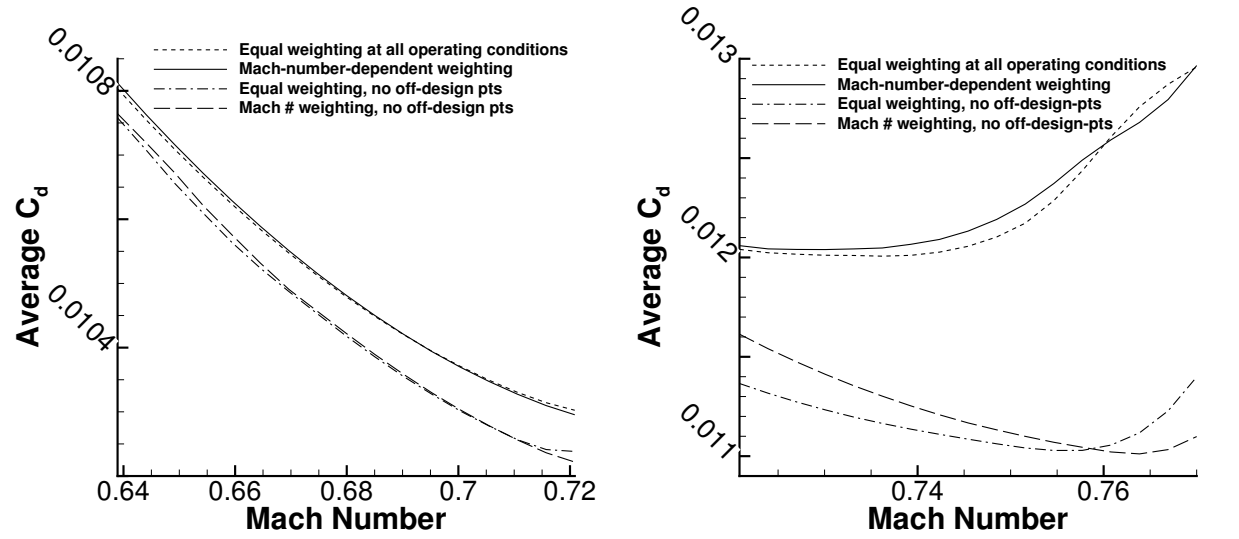

(a) Design Problem 1 (b) Design Problem 2

Figure 2. Comparison of average C_d over the range of aircraft weights versus Mach number obtained using different designer-priority weighting functions

For Design Problem 1, independent of the presence of off-design constraints, prioritizing the on-design operating conditions with a Mach-number-dependent weighting function has a negligible impact on the optimal solution. As seen in Figure 2(a), the performance of the optimal solutions obtained with each weighting function are almost identical for cases with and without off-design constraints. For this design problem with a Mach number range peaking at the low end of the transonic regime, the optimizer obtains shock-free solutions

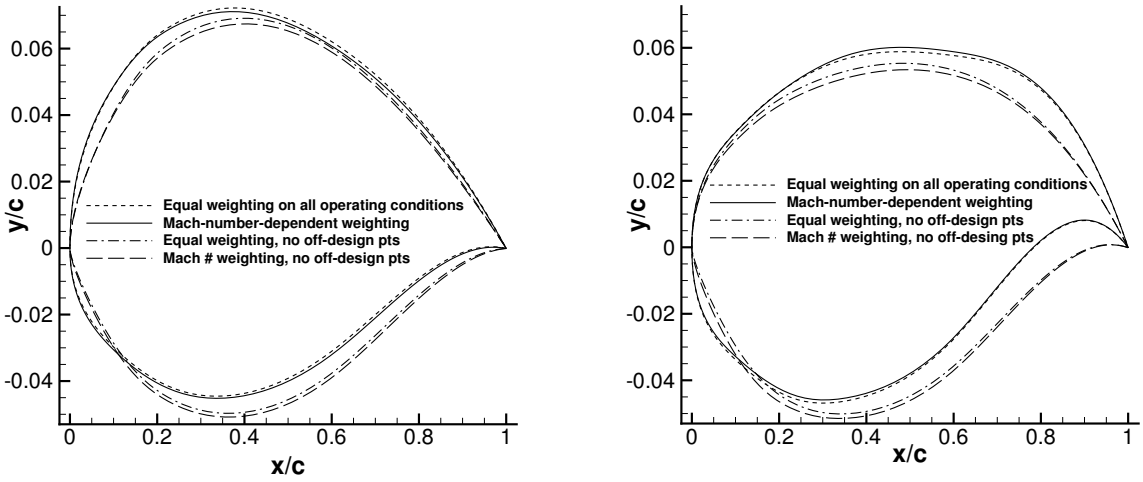

(a) Design Problem 1

(b) Design Problem 2

Figure 3. A comparison of optimal airfoil geometries obtained using different designer-priority weighting functions

over the entire range of cruise operating conditions represented by Figure 2(a). Once the shocks are eliminated, the optimal shape is driven by considerations of viscous drag, which is not sensitive to Mach number. This explains why the weighting function that is dependent on Mach number has little effect on the optimal solution in this case. Moreover, for this design case, the off-design constraints have only a small impact on on-design performance, on average less than one count of drag.

In contrast, the Mach-number-dependent weighting function has an impact on the performance of the optimal solution to Design Problem 2. For this design problem Mach numbers and lift coefficients are higher, and shocks cannot be completely eliminated for the operating conditions associated with cruise. Under these circumstances, placing more weight on higher Mach numbers does have a significant impact on the optimal solution. The cost of better performance at high Mach numbers is inferior performance over the low to mid-range Mach numbers compared to the equal weighting result. For this design problem, the weighting function gives the designer precise control over the performance of the airfoil. This enables the designer to prioritize based on the intended use of the aircraft, e.g. the proportion of time flown at specific Mach numbers. Furthermore, the weighted integral objective function, which represents performance over a range of expected operating conditions, inherently produces robust designs. As shown in Figure 2, the average C_d performance over the range of Mach numbers varies smoothly, i.e. there is no evidence of point optimization for all cases. For this design problem a substantial performance penalty is paid to satisfy the off-design constraints. It is also evident that the impact of the weighting function is reduced when the

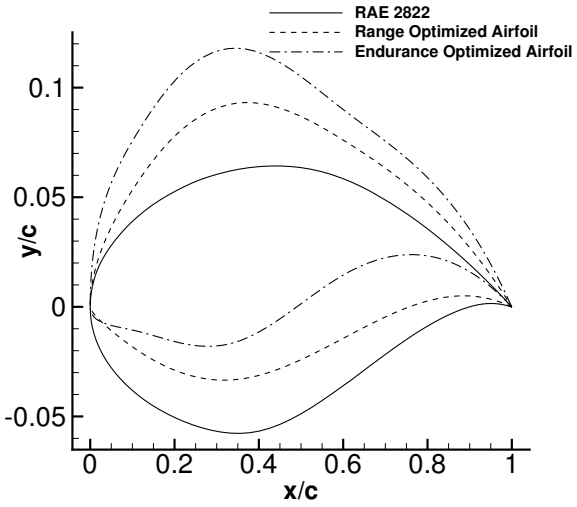

Figure 4. A comparison of UAV airfoil geometries for optimal range and endurance performance

off-design constraints are included. In this case the optimization is predominantly driven by the requirement to satisfy these constraints, thus reducing the design flexibility available to alter on-design performance.

An examination of optimized drag values over the range of on-design operating conditions shows that the maximum change in friction drag for all cases does not exceed 1.2% compared to performance for the initial airfoil geometry. Relatively small changes to friction drag are expected for airfoil optimization problems with transonic operating conditions and an assumption of fully turbulent flow. In contrast, changes to pressure drag over the course of an optimization for these cases are generally higher, with the maximum change in pressure drag exceeding 21%.

B. Range and Endurance Optimization

A series of test cases are executed to optimize the range and endurance performance of the UAV described in Section III-C and to demonstrate the advantage of using Mach number as a design variable when considering these particular performance goals. For both range and endurance objective functions, the corresponding integrals given by (6) and (7) are approximated using five quadrature points equally spaced over the range of aircraft weights. For each objective, three test cases are executed. The first is an optimization performed using only Mach number as a design variable. The optimal Mach number from the first test case is specified as a fixed value for the second test case where only geometric design variables are used. Finally an optimization is performed where both Mach number and geometric design variables are used. A comparison of airfoil geometries optimized for range and endurance

performance using both Mach number and geometric design variables is shown in Figure 4. The RAE 2822 airfoil shown on this figure is used for the test cases with only Mach number as a design variable.

Figure 5 shows a comparison of the optimized range performance obtained using the progression of design variable test cases described above. The range factor integrand is shown on the vertical axis versus the aircraft weight on the horizontal axis. The area underneath a curve in this figure represents the total range factor integral given in (6). Table 3 gives a comparison of the optimal values of the range factor integral in each case. With respect to the case where only Mach number is used as a design variable, aircraft range is improved by 1.9% for the test case where only geometric design variables are used and 2.1% for the case where both Mach number and geometric design variables are used. When using only Mach number as a design variable, the optimal Mach number, M^*, is 0.460 compared to 0.435 for the case where both Mach number and geometric design variables are used. For this design problem, the majority of improvement in aircraft range is achieved via the geometric design variables. In this case, optimizing with only geometric design variables achieves a significant improvement in range performance provided that the fixed value of Mach number used is near its optimal value. A very small additional improvement in range performance is realized by matching an optimal Mach number with an optimal shape. For this case the average changes in pressure and friction drag when comparing performance at the optimal solution to that of the initial airfoil geometry are -11.8% and -1.7% respectively.

In a similar fashion to the range optimization cases, Figure 6 shows a comparison of the optimized endurance performance obtained from the design variable test cases. Table 3 gives a comparison of the optimal values of the endurance factor integral in each case. With respect to the case where only Mach number is used as a design variable, a dramatic improvement in endurance performance of 17% is achieved by optimizing with both Mach number and geometric design variables whereas a relatively modest improvement of 5% is achieved using only geometric design variables. For the endurance optimization cases, the difference between optimal Mach numbers in each case is larger than for the range optimization cases. The fixed Mach number of 0.425 used for the case with only geometric design variables limits the improvement in endurance. For this case the average changes in pressure and friction drag when comparing performance at the optimal solution to that of the initial airfoil geometry are +14.1% and -33.7% respectively.

For both range and endurance optimizations, using Mach number and geometric design variables together produces the greatest performance improvement. Using Mach number as a design variable eliminates the need to guess an appropriate fixed value for Mach number.

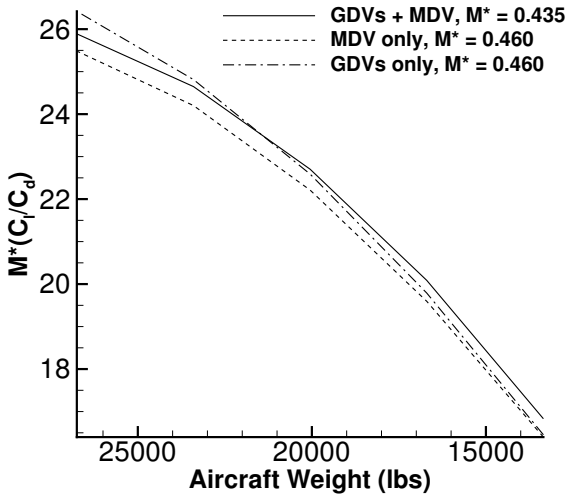

Figure 5. A comparison of UAV range performance optimized with and without Mach number as a design variable. GDV's: geometric design variables, MDV: Mach number design variable, M*: optimal Mach number

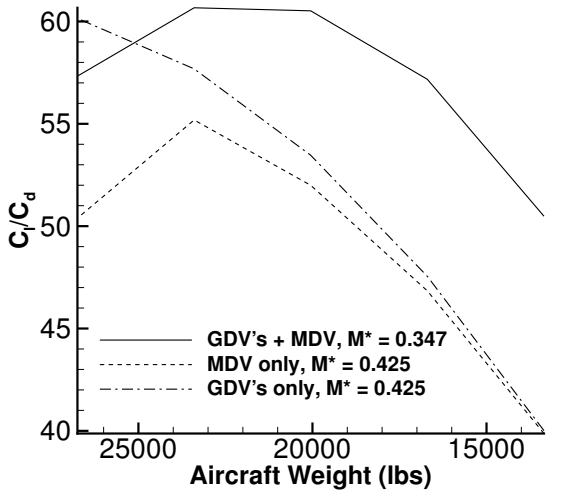

Figure 6. A comparison of UAV endurance performance optimized with and without Mach number as a design variable. GDV's: geometric design variables, MDV: Mach number design variable, M*: optimal Mach number

C. Pareto Fronts

Design via aerodynamic shape optimization can be considered an iterative process. The optimization process is capable of producing more information than simply the optimal shape. It can also provide the designer with information on various trade-offs which can be used to reformulate the objectives and constraints. The problem specification may evolve over several iterations until the final solution is a suitable compromise between all design

Design Variables	Optimal Mach Number	Range Factor Integral (lbs)	Endurance Factor Integral (lbs)
Mach number only	0.460	291323	-
geometric only	0.460 (fixed)	296978	-
geometric + Mach number	0.435	297520	-
Mach number only	0.425	-	667267
geometric only	0.425 (fixed)	-	699346
geometric + Mach number	0.347	-	778219

Table 3. Optimal UAV range and endurance integral values for test cases with and without Mach number as a design variable

objectives and constraints. In certain cases, for example Design Problem 2, experimenting with different weighting functions not only allows the designer to tailor the solution to suit mission requirements but also provides knowledge of performance trade-offs associated with prioritizing on-design operating conditions. Similarly, Pareto fronts can be used to probe the design space to yield information on any competing objectives that are of interest.

1. On-Design Performance Versus Off-Design Constraints

When considering Design Problems 1 and 2 given in Section III, a designer may be interested in the trade-off between on-design performance and off-design constraints. For Design Problem 2, the off-design constraint associated with dive conditions shown in Table 2 is $M_{max} \leq 1.35$. Setting the upper bound on $M_{ks} = 1.52$ will achieve satisfaction of this constraint at all dive operating conditions (M_{ks} is described in Section V). The Pareto front shown in Figure 7 consists of a set of optimal solutions generated by incrementally relaxing the upper bound on the M_{ks} constraint from 1.52 to 1.56. The measure of performance shown in Figure 7 is the average value of the drag coefficient over the range of Mach numbers and lift constraints for Design Problem 2 described in Section III-B. A large degradation in on-design performance is observed as the constraint upper bound becomes more restrictive. This provides the designer with precise information with respect to the impact of the off-design constraint that can be helpful if there exist alternative means of achieving the requirement addressed by the constraint. For Design Problem 1 the off-design constraint associated with low-speed conditions requires that the aircraft be capable of achieving $C_{l,max} \geq 1.60$, as shown in Table 1. The Pareto front given in Figure 8 shows the trade-off between performance at cruise conditions and the lower bound on the $C_{l,max}$ constraint at low-speed conditions. The measure of performance in this case is the average value of the drag coefficient over the range of Mach numbers and lift constraints for Design Problem 1 described in Section III-A. It can be seen that cruise performance is significantly penalized as the $C_{l,max}$ constraint is increased. The maximum drag coefficient at each point on the Pareto front

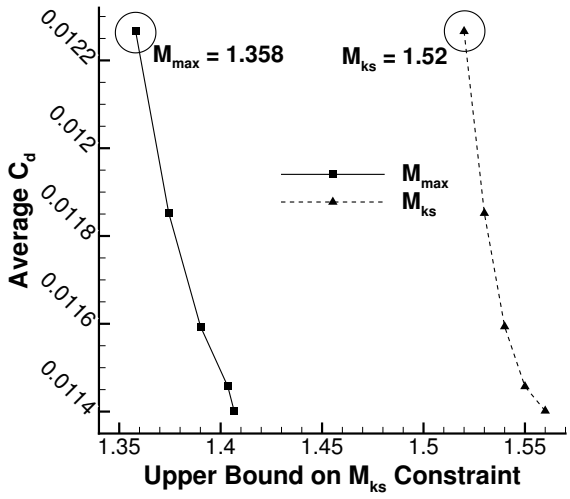

Figure 7. Trade-off between performance at cruise conditions and M_{ks} constraint at dive conditions for Design Problem 2

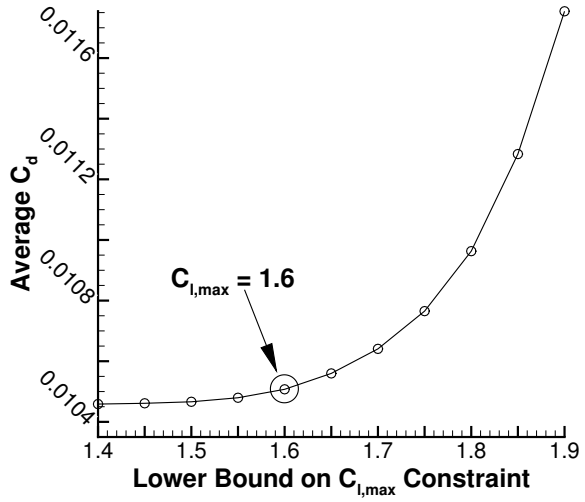

Figure 8. Trade-off between performance at cruise conditions and $C_{l,max}$ constraint at low-speed conditions for Design Problem 1

shown in Figure 8 occurs at the highest C_l and Mach number combination and varies in a manner consistent with the average C_d. Again, such quantitative information can be helpful in formulating the optimization problem.

2. Range Versus Endurance

Range and endurance are competing objectives. The range and endurance objectives are represented by two separate integrals given in (6) and (7) taken over the same range of

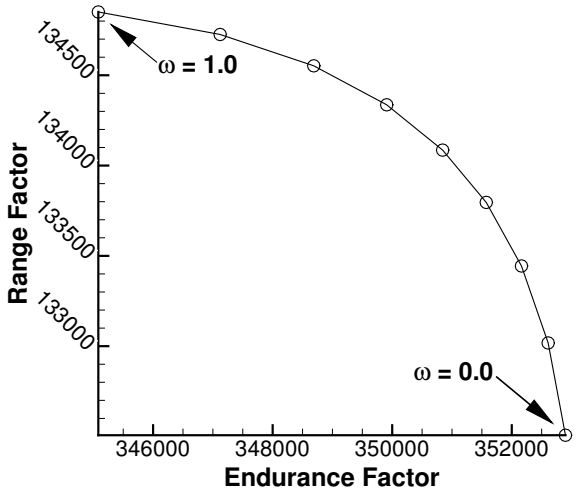

Figure 9. Trade-off between UAV range and endurance performance

aircraft weights. Two Mach number design variables are required; one for each objective. The point identified as $\omega = 1.0$ on the Pareto front shown in Figure 9 represents a design optimized for range performance. The furthest right point identified as $\omega = 0.0$ represents a design optimized for endurance performance. The intermediate designs are obtained by varying the relative weightings on the range and endurance integrals. This figure shows the trade-off in performance between range and endurance.

VII. Conclusions

Optimization performed using an objective function based on a weighted integral is an effective technique for design over a range of operating conditions. The weighted integral approach affords the designer a formal way of prioritizing based on mission requirements and leads to robust designs. Design considerations for a UAV such as aircraft range and endurance require objective functions formulated as integrals of aerodynamic quantities over a range of aircraft weights. When performing range and endurance optimizations in the absence of constraints on speed, using Mach number as a design variable in addition to geometric design variables is demonstrated to produce optimal performance. Examples of Pareto fronts are given that provide the designer with helpful information that can be used in understanding and formulating the optimization problem.

Acknowledgements

The funding of both authors by Bombardier Aerospace and the Natural Sciences and Engineering Research Council of Canada and funding of the second author by the Canada Research Chairs program is gratefully acknowledged.

Computations were performed on the GPC supercomputer at the SciNet HPC Consortium. SciNet is funded by: the Canada Foundation for Innovation under the auspices of Compute Canada; the Government of Ontario; Ontario Research Fund - Research Excellence; and the University of Toronto.

References

[1]Epstein, B., Jameson, A., Peigin, S., Roman, D., Harrison, N., and Vassberg, J., "Comparative Study of Three-Dimensional Wing Drag Minimization by Different Optimization Techniques," *Journal of Aircraft*, Vol. 46, No. 2, March-April 2009, pp. 526–541, DOI:10.2514/1.38216.

[2]Cliff, S. E., Reuther, J. J., Saunders, D. A., and Hicks, R. M., "Single-Point and Multipoint Aerodynamic Shape Optimization of High Speed Civil Transport," *Journal of Aircraft*, Vol. 38, No. 6, November-December 2001, pp. 997–1005.

[3]Zingg, D. W. and Elias, S., "Aerodynamic Optimization Under a Range of Operating Conditions," *AIAA Journal*, Vol. 44, No. 11, November 2006, pp. 2787–2792, DOI: 10.2514/1.23658.

[4]Huyse, L. and Lewis, R. M., "Aerodynamic Shape Optimization of Two-Dimensional Airfoilis Under Uncertain Operating Conditions," TM CR-2001-210648, NASA, 2001.

[5]Huyse, L., Padula, S. L., Lewis, R. M., and Li, W., "Probabilistic Approach to Free-Form Airfoil Shape Optimization Under Uncertainty," *AIAA Journal*, Vol. 40, No. 9, September 2002, DOI: 10.2514/2.1881.

[6]Li, W., Huyse, L., and Padula, S., "Robust Airfoil Optimization to Achieve Consistent Drag Reduction Over a Mach Range," *Structural and Multidisciplinary Optimization*, Vol. 24, No. 1, 2002, pp. 38–50.

[7]Buckley, H., Zhou, B., and Zingg, D. W., "Airfoil Optimization Using Practical Aerodynamic Design Requirements," *Journal of Aircraft*, Vol. 47, No. 5, September-October 2010, pp. 1707–1719, DOI: 10.2514/1.C000256.

[8]Nemec, M. and Zingg, D. W., "Newton-Krylov Algorithm for Aerodynamic Design Using the Navier-Stokes Equations," *AIAA Journal*, Vol. 40, No. 6, June 2002, pp. 1146–1154.

[9]Nemec, M., Zingg, D. W., and Pulliam, T. H., "Multipoint and Multi-Objective Aerodynamic Shape Optimization," *AIAA Journal*, Vol. 42, No. 6, June 2004, pp. 1057–1065.

[10]Gill, P. E., Murray, W., and Saunders, M. A., "SNOPT: An SQP Algorithm for Large-Scale Constrained Optimization," *SIAM Review*, Vol. 47, No. 1, February 2005, pp. 99–131.

[11]Kreisselmeier, G. and Steinhauser, R., "Systematic Control Design by Optimizing a Vector Performance Index," *International Federation of Active Controls Symposium on Computer-Aided Design of Control Systems*, Zurich, Switzerland, August 29-31 1979.

[12]Zingg, D. W., "Grid Studies for Thin-Layer-Navier-Stokes Computations of Airfoil Flowfields," *AIAA Journal*, Vol. 30, No. 10, 1992, pp. 2561–2564.

[13]Zingg, D. W., DeRango, S., Nemec, M., and Pulliam, T. H., "Comparison of Several Spatial Dis-

cretizations for the Navier-Stokes Equations," *Journal of Computational Physics*, Vol. 160, No. 2, May 2000, pp. 683–704.

[14]Nocedal, J. and Wright, S., *Numerical Optimization*, Springer, 2nd ed., 2006, pp. 320-321.

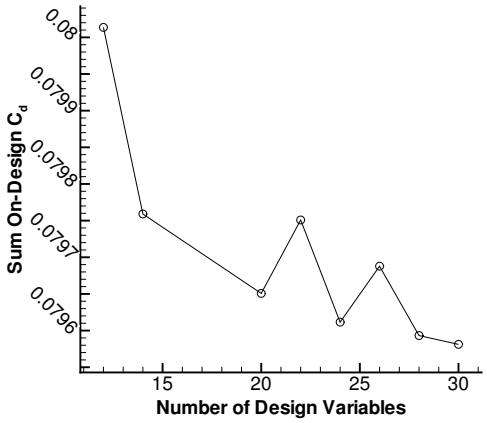

Figure 10. Sum of on-design C_d's versus number of design variables

Appendix: Selection of Parameters For Practical Aerodynamic Design Problems

A preliminary study of a design problem similar to the one described in Section III-A used an airfoil geometry parametrized by 15 B-spline control points, 12 of which were used as geometric design variables, and a grid size of 18785 nodes. These values have been revisited to study their effect on the optimal solution to the design problem. Given that computational effort increases with grid size and number of design variables, a study of these parameters aims to determine values that minimize computational effort while attaining a satisfactory solution to the design problem.

A. Design Variable Study

Optimizations were performed with number of design variables ranging from 12 to 30. Figure 10 shows a slight trend toward on-design performance improvement as the number of design variables are increased. The difference between the best and worst on-design performance, at 30 design variables and 12 design variables respectively, is approximately 0.6%. A comparison of the optimized airfoil geometries obtained with 30 design variables and 12 design variables is shown in Figure 11. The main differences in airfoil geometry are observed at the trailing edge as shown in Figure 12. The trailing edge at 30 design variables presents manufacturing and structural difficulties because it is extremely thin. The additional design variables create a requirement for some additional thickness constraints, which will reduce the already small benefit of increasing the number of design variables. Table 4 shows the number of function evaluations (where a function evaluation requires one computation of a flow solution) required as the number of design variables increases. It can be seen that the computational effort

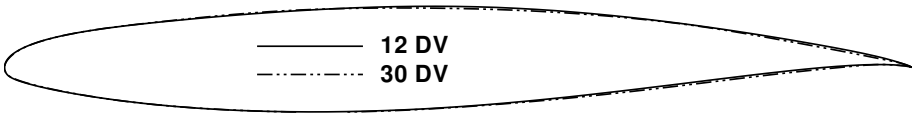

Figure 11. Comparison of optimized airfoil geometries with 12 and 30 design variables

Number of Design Variables	Number of Function Evaluations
12	47
14	41
20	141
22	133
24	134
26	152
28	164
30	232

Table 4. Number of function evaluations versus number of design variables

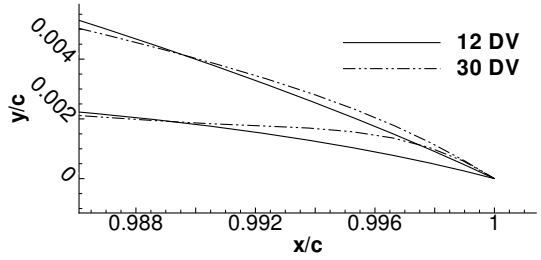

Figure 12. Comparison of optimized airfoil trailing edges with 12 and 30 design variables

increases significantly with the number of design variables. When weighing the benefit of modest performance improvements achieved with greater number of design variables against increased computational effort and infeasible airfoil geometry with respect to manufacturing and structural concerns, using 12-14 design variables is recommended, as values in this range provide a sufficiently optimal solution to this design problem and will likely be suitable for design problems with similar operating conditions.

B. Grid Density Study

To investigate the effect of grid size on the optimal solution, optimizations are performed using the coarse and fine grids described in Table 5. Performance of the optimal solution at each grid size is evaluated using the evaluation grid, which is extremely fine and produces very accurate lift and drag coefficients. Design problem 1 described in Section III-A is used

as the test case.

An iterative optimization procedure is required to ensure that active off-design constraints are comparably satisfied at optimal solutions for each grid size when evaluated on the evaluation grid. This is because the values of the constraint bounds at each grid that will satisfy the constraints when evaluated on the evaluation grid are not known beforehand. Design Problem 1 described in Section III-A specifies that the maximum Mach number at dive conditions 1 - 8 must not exceed 1.35 and that $C_{l,max} \geq 1.778$ at high-lift conditions 9 - 10. It is known that our flow solver will under-predict these constraint values in proportion to the grid size. To address this issue, an initial guess for the constraints is used at each grid size. The initial guess is based on evaluation of the constraints at the initial geometry using both the coarse grid and the evaluation grid. A converged optimal solution is obtained using the initial guess for the constraint bounds. The constraints are evaluated using the optimal solution on the evaluation grid. The constraint bounds are updated according to the following formulas and used for the next optimization iteration:

$$\left(C^*_{l,max}\right)^{n+1}_{(C)} = \left(C^*_{l,max}\right)_{(E)} - \left[(C_{l,max})^n_{(E)} - (C_{l,max})^n_{(C)}\right] \tag{11}$$

$$(M^*_{max})^{n+1}_{(C)} = (M^*_{max})_{(E)} - \left[(M_{max})^n_{(E)} - (M_{max})^n_{(C)}\right] \tag{12}$$

Subscripts C and E denote constraint evaluations on coarse grids and the evaluation grid respectively and the superscript is the index of optimization iterations. $(C^*_{l,max})^n_{(C)}$ is the lower bound on the high lift constraint used on the coarse grid at optimization iteration n. $(C^*_{l,max})_{(E)}$ is the lower bound on the high lift constraint used on the evaluation grid. This is the constraint value we are trying to achieve, i.e. $C_{l,max} \geq 1.778$. $(C_{l,max})^n_{(E)}$ is the value of the high lift constraint evaluated on the evaluation grid at optimization iteration n. $(C_{l,max})^n_{(C)}$ is the value of the high lift constraint evaluated on the coarse grid at optimization iteration n. An analogous naming convention is used in the M_{max} constraint bound update formula.

After three optimization iterations the constraints for optimal solutions at each grid are satisfied to within a tolerance of ± 0.005 when evaluated on the evaluation grid. Table 6 shows a comparison of the sum of drag coefficients at on-design operating conditions evaluated using the evaluation grid with the optimal solution at each grid size. A comparison of the active off-design constraints evaluated using the evaluation grid with the optimal solution at each grid size is also given in Table 6. Figure 13 shows a comparison of the optimal geometries at each grid size. A 1% performance improvement in the optimal solution has been achieved using the fine grid versus the coarse grid. A slight difference in the optimal geometries is visible.

Grid Name	Size	Off-wall Spacing (chord)
coarse	289×65	2.0×10^{-6}
fine	401×89	2.0×10^{-6}
evaluation	917×193	7.5×10^{-7}

Table 5. Grids used to study the effect of grid density on the optimal solution

Grid Name	Sum of On-Design C_d	$(C_{l,max})_{(E)}$	$(C^*_{l,max})_{(C)}$	$(M_{max})_{(E)}$	$(M^*_{max})_{(C)}$
coarse	0.06632	1.778	1.5706	1.355	1.281
fine	0.06566	1.779	1.628	1.352	1.301

Table 6. Comparison of on-design performance and active off-design constraints computed on the evaluation grid for optimal solutions obtained with three different grid sizes

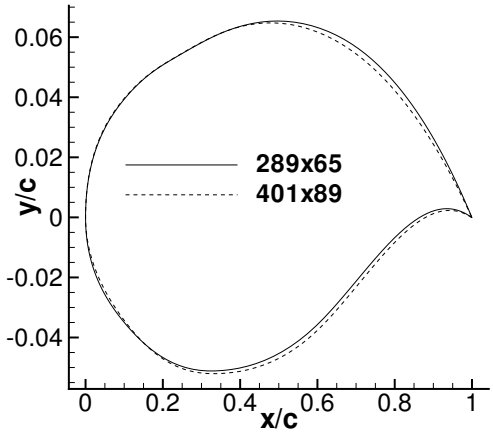

Figure 13. Comparison of optimal airfoil geometries obtained using different grid densities

C. Determination of Maximum Mach Number Constraint Bound M^*_{ks}

As described by Buckley et. al[7] and reviewed in Section V, the KS function provides a conservative estimate of the maximum Mach number in the flow field that is used as the basis for the maximum Mach number constraint associated with dive conditions. At dive conditions, $M_{max} \leq M^*_{max}$. M^*_{ks} is defined as the bound on the conservative estimate of maximum Mach number based on the KS function. M^*_{max} is the actual bound on maximum Mach number in the flow field. M_{max} is the maximum Mach number evaluated at the optimal solution. At an optimal solution, SNOPT ensures that M_{ks} at all dive conditions does not exceed M^*_{ks}. It is not known beforehand what value of M^*_{ks} will produce $M_{max} \leq M^*_{max}$. The iterative procedure described below is used to obtain the appropriate value of M^*_{ks} for a given design problem:

1. Start with an initial guess for M^*_{ks}: $M^*_{ks} = M^0_{ks}$

2. Run the optimization until a converged solution is obtained

3. Calculate the discrepancy in M_{max} : $\Delta M_{max} = M^*_{max} - M_{max}$

4. Update guess for M^*_{ks}: $M^*_{ks} = M^1_{ks} = M^0_{ks} + \Delta M_{max}$

5. Restart the optimization using updated value for M^*_{ks}

6. Repeat steps 2 - 5 until $M_{max} \simeq M^*_{max}$ at the converged solution to within some specified tolerance

The maximum Mach number constraint can be satisfied to within $\pm 1 \times 10^{-4}$ in 5 iterations.